Published in final edited form as:
Carbon N Y. 2010 June 1; 48(7): 1961–1969. doi:10.1016/j.carbon.2010.02.002.

Biodurability of Single-Walled Carbon Nanotubes Depends on Surface Functionalization

Xinyuan Liu[1], **Robert H. Hurt**[2,4,*], and **Agnes B. Kane**[3,4]

[1] Department of Chemistry, Brown University, Providence, Rhode Island [2] Division of Engineering, Brown University, Providence, Rhode Island [3] Department of Pathology and Laboratory Medicine, Brown University, Providence, Rhode Island [4] Institute for Molecular and Nanoscale Innovation, Brown University, Providence, Rhode Island

Abstract

Recent research has led to increased concern about the potential adverse human health impacts of carbon nanotubes, and further work is needed to better characterize those risks and develop risk management strategies. One of the most important determinants of the chronic pathogenic potential of a respirable fiber is its biological durability, which affects the long-term dose retained in the lungs, or biopersistence. The present article characterizes the biodurability of single-walled carbon nanotubes using an in vitro assay simulating the phagolysosome. Biodurability is observed to depend on the chemistry of nanotube surface functionalization. Single-walled nanotubes with carboxylated surfaces are unique in their ability to undergo 90-day degradation in a phagolysosomal simulant leading to length reduction and accumulation of ultrafine solid carbonaceous debris. Unmodified, ozone-treated, and aryl-sulfonated tubes do not degrade under these conditions. We attribute the difference to the unique chemistry of acid carboxylation, which not only introduces COOH surface groups, but also causes collateral damage to the tubular graphenic backbone in the form of neighboring active sites that provide points of attack for further oxidative degradation. These results suggest the strategic use of surface carboxylation in nanotube applications where biodegradation may improve safety or add function.

1. Introduction

A major concern in the emerging field of nanotechnology is the analogy between asbestos fibers and carbon nanotubes with respect to their diameter, aspect ratio, high surface area, and biopersistence [1,2]. Rodent toxicology assays have demonstrated the potential for carbon nanotubes to induce inflammation [3], fibrosis [4], and malignant mesothelioma [5] similar to asbestos fibers [6]. Inhalation is a likely route for human exposure to aerosolized engineered nanomaterials in the workplace [7–9] raising significant concerns about safety in the nanotechnology industry [10].

Chronic rodent inhalation assays using asbestos and man-made mineral fibers have correlated fiber length and biopersistence with induction of inflammation, fibrosis, lung cancer, and

*Corresponding author. Fax: +401 8639120. Robert_Hurt@brown.edu (R.H. Hurt). Fax: +401 8639120. Agnes_Kane@brown.edu (A.B. Kane).

malignant mesothelioma [11]. Macrophages are the initial target cell for particulates inhaled into the lungs; particulates and microbes are rapidly engulfed by phagocytosis and cleared up the mucociliary escalator or via lymphatics to regional lymph nodes [12]. Following phagocytosis, the phagosome fuses with lysosomes within the cell to form an acidic, membrane-bound phagolysosome [13]. Macrophages also generate oxidants including superoxide anion, hydrogen peroxide, and hydroxyl radical that contribute to microbial killing in the phagolysosome [14]. Biopersistence is defined as the dose of particulates retained in the lungs following deposition and clearance by macrophages and chemical degradation [12]. Macrophage-mediated clearance is related to deposited dose and fiber dimensions [15] and for mineral fibers, chemical dissolution in the lungs is determined by crystallinity, chemical composition, and surface area [16]. Biopersistence is assessed by retention kinetics following short-term intratracheal instillation or inhalation of particulates by rodents [11].

A fundamental material property that influences biopersistence is “biodurability” -- the long-term chemical stability in biological compartments. Dissolution and/or degradation alters the biological distribution and fate of foreign materials in the body [17], and for mineral fibers this biodurability is commonly assessed by measuring dissolution rates in macrophage cultures [18] or in cell-free chemical assays [19].

For carbon nanotubes, there is little information on their biodurability, though they belong to the family of graphenic carbon materials (defined as those composed primarily of carbon in sp^2-hybridized bonding states, or, equivalently, those formed from sets of flat, curved, or distorted graphene layers), which are generally quite stable in environmental and biological media. The approach used for mineral fibers measuring initial rates of dissolution is not well suited to graphenic carbon materials, because they do not dissolve at measurable rates in typical physiological aqueous phases. Although graphenic carbon does not dissolve, it can in principle be oxidized, and several recent studies have examined SWCNT persistence/degradation in mild oxidative environments. Liu et al. [20] report that SWCNT samples did not undergo significant morphological changes in a 60-day assay using a flow-through solution containing 1 mM H_2O_2, iron salts, and ascorbic acid for the continuous generation of hydroxyl radicals. The goal was to determine if this medium, designed to simulate the acidic and oxidizing environment in late-stage endosomes or phagolysosomes [21] could attack carbon shells in the SWCNT sample and create defects allowing fluid access and release of Ni^{2+} from the underlying metal catalyst particle. Allen et al. [22] were the first to report conditions under which SWCNT samples show biodegradation. Using an environmental model system containing 40 uM H_2O_2 and horseradish peroxidase, Allen et al. show tube length reduction and debris accumulation after 12 weeks. The different observations in the Liu et al. study (durability) and the Allen et al. study (biodegradation), may be related to differences in nanotube samples, media, or the presence of an exogenous enzyme.

Here we systematically investigate the role of carbon nanotube surface functionalization in the biodurability of carbon nanotubes in a mild, physiologic oxidizing environment. We focus on simulating the phagolysosomal compartment which is relevant for the interaction of nanotubes with macrophages in the lung, pleura, or peritoneum [11] and examine a range of common nanotube surface functionalization methods.

2. Experimental

2.1. Materials

This study used a panel of commercial single-walled carbon nanotubes (SWCNTs) both as-received and subjected to surface functionalization based on ozonolysis, aryl-sulfonation, and acid carboxylation (see Table 1). Ozonolysis was carried out by placing 12.6 mg of nanotubes in a quartz tube on a fritted silica filter, and introducing 1 L/min of 0.24 wt% ozone in air

generated using a CD10/AD corona discharge system (Clearwater Tech. Inc.) for 20 min. Aryl-sulfonation was carried out using sulfanilic acid and sodium nitrite in aqueous solution at 70 °C as described by Yan et al. [23]. Carboxylation was carried out by agitating ca 60 mg nanotubes in 100ml mixed acid solutions (98% H_2SO_4: 70% HNO_3=3:1) for 15min, 1hr and 3hrs. An additional SWCNT-COOH sample was obtained commercially following post synthesis treatment with nitric acid (vendor-reported). As reference materials, we included 200 nm-diameter platelet-symmetry carbon nanofibers [24], and positive and negative mineral fiber controls. As a negative control for durability we used wollastonite, a soluble calcium silicate fiber that does not induce persistent inflammation, fibrosis, or lung cancer [25,26]. For a positive control, we used crocidolite asbestos fibers, which are highly biopersistent and induce chronic inflammation, fibrosis, lung cancer, and malignant mesothelioma in rodents and humans [11].

2.2. Biodurability assay

Nanotubes or reference materials (2.0–2.5 mg) were placed in a 15 ml Corning graduated tube covered with alumina foil containing 8–10 ml of a phagolysosomal simulant fluid (PSF) described by Stefaniak et al. [21], which is designed to mimic the low pH and chemical environment of phagolysosome where nanomaterials are localized intracellularly following phagocytosis. The PSF (pH 4.5) consists of Na_2HPO_4, NaCl, Na_2SO_4, $CaCl_2{\cdot}2H_2O$, glycine, potassium hydrogen phthalate buffer salts and alkylbenzyldimethylammonium chloride as an antifungal agent. To create a simulated physiological oxidizing environment, H_2O_2 at a typical physiological concentration of 1 mM was added [14,20] was added and the mixture subjected to mild bath sonication for 1hr followed by gentle rotation at 60 rpm in the dark for 90 days. During this incubation period, additional H_2O_2 was added once a week in an amount equivalent to reproduce 1 mM concentration in the remaining solution (which was determined by the remaining liquid volume and that was addition of 50–100ul of 100mM peroxide solution). After different incubation times (1, 7, 30, 60, 90 days), the suspensions were sonicated and vortexed to achieve uniformity, then a 1 ml aliquot was removed and transferred to a filtration centrifuge tube (3000 NMWL Amico centrifugal filter devices, Millipore, MA) and subjected to 30–60 min of centrifugation prior to characterization.

2.3. Characterization

Morphology and tube dimensions of the filtered solids were characterized by transmission electron microscopy (Philips 420 at 120 kV) and field-emission scanning electron microscopy (LEO 1530 FE-SEM) by re-suspension in ethanol and drying, and by dynamic light scattering (Zetasizer Nano-ZS, Malvern Instruments, Inc) by re-suspension in dimethylformamide (DMF). SEM specimens were prepared by bar-coating well-dispersed SWCNTs suspensions on silicon substrates. To determine tube length distribution statistics, ca. 220–340 individual tubes were identified on TEM or SEM micrographs for each sample and measured by hand counting using the image processing program, *ImageJ*. The optical properties of the filtrates were also studied by fluorescence spectroscopy (QuantaMaster QM-4 Luminescence Spectrometer, Photon Technology International, Inc.).

3. Results

The 12 nanotube and reference fiber samples assembled for this study behaved quite differently upon long-term exposure to an oxidizing phagolysosomal simulant fluid. Crocidolite asbestos, a positive control for biodurability, showed no apparent changes after 90 days, as expected. The negative control, wollastonite, was completely dissolved at the point of first inspection (30 days), consistent with its low biopersistence reported by Warheit et al. and Macdonald et al.[25,26].

The carbon nanotube samples showed considerable variation depending on type and functionalization. Most nanotube samples showed little change when examined by TEM, as illustrated in Figure 1. This unfunctionalized sample consisted of a nearly continuous network of entangled SWCNT ropes that was unaffected by 90 day mild agitation in the oxidizing, low-pH biological stimulant fluid (see Fig. 1). Other SWCNT samples showed subtle or modest changes in aggregation state reflecting gradual disentanglement of the ropes, especially the hydrophilic tube samples functionalized with aryl-sulfonate or ozone, but no evidence of length reduction by tube cutting.

Figure 2 shows that carboxylated SWCNTs exhibit a very different behavior. They undergo extensive breakup of the entangled rope networks and liberation of short tubes or tube bundles that become progressively shorter by chemical attack on the tubular graphene during incubation. SEM images provide more information on the morphological evolution of carboxylated SWCNTs. For SEM analysis the CNTs were dispersed from ethanol suspensions onto silicon substrates by bar-coating (see example, Fig. 3a). Figure 3 panel b and c show nanotube length distributions determined by manual measurement and counting of about three hundred individual tubes identified on SEM micrographs for the SWCNT-COOH samples. It is evident that shorter nanotubes are significantly more abundant after 90-day exposure to the physiological oxidizing environment (c) relative to the original SWCNTs (b). Histograms derived from TEM images also show tube shortening after 90 day exposure (data not shown).

Dynamic light scattering is useful as a qualitative tool to track changes in size and aggregation state in situ – without the need for drying or substrate deposition. The annealed, low-functional-group nanotubes in Fig. 1 show a bimodal size distribution, which we interpret as the presence of continuous entangled rope structures (the 3–8 um large aggregate peak) coexisting with primary tubes/bundles any equi-axed particulate carbon by-products (the 50 – 800 nm peak), which are free in suspension and not connected to the large entangled rope networks. For most of the nanotube samples studied, the bimodal distribution shows few or modest changes (see Fig. 1c), whereas the carboxylated tubes show highly significant changes in the distribution of both peak heights and locations (Fig. 4). Over time, the SWCNT-COOH large-aggregate peak loses intensity and by 90 days disappears, reflecting the near total loss of the entangled rope networks. In its place the free primary peak grows, and the peak shifts to progressively smaller sizes (Fig. 4a). Because DLS estimates hydrodynamic size, it is sensitive to changes in aggregation, length reduction, and the breakup of the primary bundles or ropes, which reduces their apparent diameter. The migration of the peak location thus provides a crude measure of the extent of primary tube debundling in combination with shortening (Fig. 4c), while the decrease in large-aggregate peak height provides a measure of disentanglement or large network structures (Fig. 4b). DLS size analysis relies on spherical geometry, so cannot be used to provide the primary data on length reduction in this study. That evidence comes from electron microscopy rather (Fig. 2 and 3), but DLS is nevertheless useful to track the physical evolution of the samples in situ.

Carboxylation is typically carried out by treatment with oxidizing acids, HNO_3 and H_2SO_4, alone or in mixtures, or in combination with peroxide [27–29]. In this study, similar behavior was observed with the commercial sample (carboxylated with HNO_3) and samples treated in-house with HNO_3/H_2SO_4 for 1 or 3 hrs (see Table 1).

Control experiments were carried out by incubating carboxylated SWCNTs in DI H_2O, only PSF medium, or only 1mM H_2O_2 with mild agitatition for 90 days. As shown in Figure 5, there is no evident tube shortening or degradation following incubation in either water (Fig. 5a) or PSF medium (Fig. 5b), whereas long, entangled carboxylated tubes subjected to 90 days treatment degraded into short tubes or debris after exposure to 1mM H_2O_2 (Fig. 5c) or 1mM

H_2O_2 plus PSF (Fig. 5d), suggesting that continuous exposure to an oxidizing environment is important for further attack and degradation of SWCNTs-COOH.

The large changes in morphology for the SWCNT-COOH samples were accompanied by accumulation of solid particulate debris (Fig. 6). Note that all of the samples contain some equi-axed carbon solids, which in the fresh samples include graphenic carbon shells originally templated on catalyst particles and often found at tube tips. After 90 day exposure of the SWCNT-COOH samples, however, one sees accumulation of additional globular material that appears on tube walls and dispersed throughout the sample in dried SEM specimens as shown in Figure 6. This debris suggests a chemical degradation process rather than a simple tube cutting and disentanglement by the mild mechanical forces generated by slow sample rotation.

To test the hypothesis of chemical degradation, we examined the UV-visible spectral characteristics of the clear filtrates following removing of the nanotubes using centrifugal ultrafiltration with a 3000 NMWL (ca 2nm) pore cellulose membrane. Figure 7 shows that the ultra-filtrates of the 90-day exposed SWCNT-COOH samples are strongly fluorescent under 365 nm illumination. Neither the simulant fluid itself, nor the ultrafiltrates from fresh nanotube suspension were fluorescent, indicating that the fine (< 2 nm) fluorescent products appear during the 90 day treatment. Figure 7 also shows the excitation and fluorescence spectra, centered at 300 nm and 405 nm, respectively. Other SWCNT types (unfunctionalized, ozone treated, and aryl-sulfonated) exposed to phagolysosomal stimulant for 90 days do not exhibit strong fluorescence in their ultrafiltrates (Fig. 7b), indicating again that the SWCNT-COOH sample is unique in its ability to undergo chemical degradation under these conditions. We suspect that the fluorescent degradation products are primarily carbonaceous nanoparticles (< 2nm), which have been reported to exhibit fluorescence [30–32]. The excitation (250–300 nm) and fluorescence (400–450 nm) spectra are similar to those reported for graphenic material with polyaromatic substructures [33].

4. Discussion

The significant finding in this study is that SWCNTs carboxylated by treatment with oxidizing acids (HNO_3 or HNO_3/H_2SO_4) degrade after 90 days in a mildly oxidizing phagolysosomal stimulant fluid, while unmodified SWCNTs and those functionalized by ozonolysis or aryl-sulfonation do not. The accumulation of carbonaceous debris and the appearance of < 2nm fluorescent material in the ultra-filtrates both suggest a chemical degradation process. What is unique about carboxylation that renders SWCNT-COOH unstable to further degradation in mild oxidizing physiological media? The instability of SWCNT-COOH cannot be related simply to hydrophilicity and improved fluid contact during rotation, as the aryl-sulfonation treatment produces the most hydrophilic samples, but does not cause tube shortening or degradation products.

We propose that the instability of SWCNT-COOH is related to collateral damage to the tubular graphenic backbone that is intrinsic to acid carboxylation. Figure 8 shows a selection of sidewall functional groups relevant to this study. Aryl-sulfonation is an addition reaction that forms one bond attached to a backbone carbon atom, which disrupts the pi-conjugation at that site, but still allows three bonds to neighboring atoms in the backbone. Oxidative treatments produce a variety of functional groups including epoxide, peroxide, hydroxyl, carbonyl, and carboxylate. Ozonolysis forms epoxides or ozonides, the latter typically decomposing to stable carbonyl groups [34,35]. Epoxide, hydroxyl, and some (closed) peroxides are addition products, which like aryl-sulfonate, disrupt local pi-conjugation but allow three backbone bonds to remain. Carboxylation, however, requires formation of three bonds to the participating carbon atom, and since the reagents (HNO_3, H_2SO_4, H_2O_2) contain no carbon, the carbon atom must come from the nanotube itself, leaving it attached to the graphenic backbone by only one

bond. (Carbonyl groups show intermediate behavior with two backbone bonds remaining.) Thus carboxylation breaks two backbone C-C bonds and leaves two active sites adjacent to the COOH (see Fig. 8) group, which can be the sites for further oxidative attack [36]. The ability of HNO_3 or HNO_3/H_2SO_4 to damage and even consume graphenic carbon is well known; H_2O_2 or O_3 (ozone) are preferred reagents for introducing oxygen-containing functional groups on activated carbon surfaces without destruction of the graphenic structures and loss of surface area [29,37]. Further, in the present experiments, treatment of SWCNTs at times longer than 5hr destroys the tubular graphene and converts it to flake-like or globular carbonaceous debris. Carboxylation by oxidizing acids represents the early stages of this tube destruction, and the two new active sites created for each COOH group render the material less stable to further oxidation and ultimate tube cutting in phagolysosomal simulant fluid.

There are few in vivo studies to which we can meaningfully compare the present data. Lam et al reported that SWCNTs are insoluble and non-biodegradable in mice after 90 days exposure [38], and Yang et al found that acid washed SWCNTs are intact and stable in mice organs from TEM after 1 day post exposure [39].” The most interesting comparison to our data is that of Allan et al. [22]. That study showed biodegradation of SWCNTs under environmental conditions containing 40 uM H_2O_2 and the enzyme horseradish peroxidase for 12 weeks at 4 °C. For comparison, the present study used a physiological simulant of the phagolysosome, a biological compartment relevant to fiber/macrophage interactions in the lung, pleura, or peritoneum with a 25-fold higher peroxide concentration (1 mM), higher temperature (20 °C), lower pH (4.5), mild agitation, the absence of an enzyme, and a different salt composition (KHP vs. phosphate buffer). An important aspect of the comparison is that both studies report degradation of carboxylated nanotubes. The oxidizing acid mixture used to purify the tubes in the Allen et al. study (H_2SO_4/H_2O_2) is known to impart carboxylate groups, as pointed out by the original authors [22]. That sample is most closely comparable to the HNO_3 or H_2SO_4/HNO_3 SWCNTs used in the present study, which all show degradation. Allen et al. report no degradation of SWCNT-COOH in the absence of the enzyme, which might be seen as inconsistent with the present study, however, the non-enzymatic conditions used here are harsher in many respects (pH, peroxide concentration, temperature, time). Overall, both studies are consistent, in that they both show chemical degradation of SWCNT-COOH in mild oxidizing media, the contribution of the present paper being the finding that this behavior is unique to the carboxylated sample and not a general property of SWCNTs, at least in the absence of enzyme.

Returning to the asbestos analogy [40], it is known that mineral fibers can be altered by chemical leaching, dissolution, transverse breakage, or longitudinal splitting in the lungs [16]. Chemically-leached or corroded mineral fibers are broken into shorter fibers that are more readily phagocytized and cleared by macrophages [11]. Carboxylated single-walled carbon nanotubes in this simulated phagolysosomal assay showed both longitudinal splitting or debundling as well as oxidative degradation of the side walls producing ultrafine carbonaceous particles. We therefore anticipate by analogy that these oxidatively-degraded carbon nanotubes may be more readily cleared from the lungs and induce less toxicity than native or other types of surface-functionalized single-walled carbon nanotubes. These results provide proof-of-principle for intelligent design of functionalized carbon nanotubes for selective drug targeting and drug delivery [41,42] with decreased biopersistence and minimal potential for long-term adverse health effects. The results also opens the possibility to engineer SWCNTs as biomedical implant components [43] that stimulate or guide growth of tissue (e.g. nerve, muscle) and then undergo programmed degradation to prevent chronic pathologic reactions triggered by the foreign implant. For other applications where uniform dispersion and high stability in aqueous phases are desired, acid carboxylation is not a desirable functionalization scheme and aryl-sulfonation or other addition chemistries involving hydrophilic terminal groups are preferred.

Acknowledgments

Financial support was provided by the NIEHS through grants R01 ES016178 and the Superfund Research Program P42 ES013660, and the National Science Foundation (NIRT grant DMI-0506661). While this work was supported financially in part by the NIEHS, the article does not necessarily reflect the views of the agency. The technical contributions of Indrek Kulaots are gratefully acknowledged.

References

1. Donaldson K, Aitken R, Tran L, Stone V, Duffin R, Forrest G, et al. Carbon nanotubes: A review of their properties in relation to pulmonary toxicology and workplace safety. Toxicol Sci 2006;92(1):5–22. [PubMed: 16484287]
2. Kane AB, Hurt RH. Nanotoxicology: The asbestos analogy revisited. Nat Nanotechnol 2008;3(7):378–9. [PubMed: 18654556]
3. Poland CA, Duffin R, Kinloch I, Maynard A, Wallace WAH, Seaton A, et al. Carbon nanotubes introduced into the abdominal cavity of mice show asbestos-like pathogenicity in a pilot study. Nat Nanotechnol 2008;3(7):423–8. [PubMed: 18654567]
4. Card JW, Zeldin DC, Bonner JC, Nestmann ER. Pulmonary applications and toxicity of engineered nanoparticles. Am J Physiol-Lung C 2008;295(3):L400–L11.
5. Takagi A, Hirose A, Nishimura T, Fukumori N, Ogata A, Ohashi N, et al. Induction of mesothelioma in p53+/− mouse by intraperitoneal application of multi-wall carbon nanotube. J Toxicol Sci 2008;33 (1):105–16. [PubMed: 18303189]
6. Sanchez VC, Pietruska JR, Miselis NR, Hurt RH, Kane AB. Biopersistence and potential adverse health impacts of fibrous nanomaterials: What have we learned from asbestos? Wiley Interdisciplinary Reviews: Nanomedicine 2009;1:511–529.
7. Maynard AD, Baron PA, Foley M, Shvedova AA, Kisin ER, Castranova V. Exposure to carbon nanotube material: Aerosol release during the handling of unrefined single-walled carbon nanotube material. J Toxicol Env Heal A 2004;67(1):87–107.
8. Han JH, Lee EJ, Lee JH, So KP, Lee YH, Bae GN, et al. Monitoring multiwalled carbon nanotube exposure in carbon nanotube research facility. Inhal Toxicol 2008;20(8):741–9. [PubMed: 18569096]
9. Demou E, Peter P, Hellweg S. Exposure to Manufactured Nanostructured Particles in an Industrial Pilot Plant. Ann Occup Hyg 2008;52(8):695–706. [PubMed: 18931382]
10. Stern ST, McNeil SE. Nanotechnology safety concerns revisited. Toxicol Sci 2008;101(1):4–21. [PubMed: 17602205]
11. Bernstein D, Castranova V, Donaldson K, Fubini B, Hadley J, Hesterberg T, et al. Grp IRSIW. Testing of fibrous particles: Short-term assays and strategies - Report of an ILSI risk science institute working group. Inhal Toxicol 2005;17(10):497–537. [PubMed: 16040559]
12. Oberdorster G, Oberdorster E, Oberdorster J. Nanotoxicology: An emerging discipline evolving from studies of ultrafine particles. Environ Health Persp 2005;113(7):823–39.
13. Kinchen JM, Ravichandran KS. Phagosome maturation: going through the acid test. Nat Rev Mol Cell Bio 2008;9(10):781–95. [PubMed: 18813294]
14. Fang FC. Antimicrobial reactive oxygen and nitrogen species: Concepts and controversies. Nat Rev Microbiol 2004;2(10):820–32. [PubMed: 15378046]
15. Oberdorster G. Significance of particle parameters in the evaluation of exposure-dose-response relationships of inhaled particles. Particul Sci Technol 1996;14(2):135–51.
16. Fubini B. Surface reactivity in the pathogenic response to particulates. Environ Health Persp 1997;105:1013–20.
17. Borm P, Klaessig FC, Landry TD, Moudgil B, Pauluhn J, Thomas K, et al. Research strategies for safety evaluation of nanomaterials, Part V: Role of dissolution in biological fate and effects of nanoscale particles. Toxicol Sci 2006;90(1):23–32. [PubMed: 16396841]
18. Nguea HD, de Reydellet A, Le Faou A, Zaiou M, Rihn B. Macrophage culture as a suitable paradigm for evaluation of synthetic vitreous fibers. Crit Rev Toxicol 2008;38(8):675–95. [PubMed: 18686077]

19. de Meringo A, Morscheidt C, Thelohan S, Tiesler H. In-Vitro Assessment of Biodurability - Acellular Systems. Environ Health Persp 1994;102:47–53.
20. Liu X, Guo L, Morris D, Kane AB, Hurt RH. Targeted removal of bioavailable metal as a detoxification strategy for carbon nanotubes. Carbon 2008;46(3):489–500. [PubMed: 19255622]
21. Stefaniak AB, Guilmette RA, Day GA, Hoover MD, Breysse PN, Scripsick RC. Characterization of phagolysosomal simulant fluid for study of beryllium aerosol particle dissolution. Toxicol in Vitro 2005;19(1):123–34. [PubMed: 15582363]
22. Allen BL, Kichambare PD, Gou P, Vlasova II, Kapralov AA, Konduru N, et al. Biodegradation of Single-Walled Carbon Nanotubes through Enzymatic Catalysis. Nano Lett 2008;8(11):3899–903. [PubMed: 18954125]
23. Yan AH, Xiao XC, Kulaots I, Sheldon BW, Hurt RH. Controlling water contact angle on carbon surfaces from 5 degrees to 167 degrees. Carbon 2006;44(14):3116–20.
24. Chan C, Crawford G, Gao YM, Hurt R, Jian KQ, Li H, et al. Liquid crystal engineering of carbon nanofibers and nanotubes. Carbon 2005;43(12):2431–40.
25. Warheit DB, Hartsky MA, Mchugh TA, Kellar KA. Biopersistence of Inhaled Organic and Inorganic Fibers in the Lungs of Rats. Environ Health Persp 1994;102:151–7.
26. Macdonald JL, Kane AB. Mesothelial cell proliferation and biopersistence of wollastonite and crocidolite asbestos fibers. Fund Appl Toxicol 1997;38(2):173–83.
27. Liu J, Rinzler AG, Dai HJ, Hafner JH, Bradley RK, Boul PJ, et al. Fullerene pipes. Science 1998;280 (5367):1253–6. [PubMed: 9596576]
28. Hu H, Bhowmik P, Zhao B, Hamon MA, Itkis ME, Haddon RC. Determination of the acidic sites of purified single-walled carbon nanotubes by acid-base titration. Chem Phys Lett 2001;345(1–2):25–8.
29. Datsyuk V, Kalyva M, Papagelis K, Parthenios J, Tasis D, Siokou A, et al. Chemical oxidation of multiwalled carbon nanotubes. Carbon 2008;46(6):833–40.
30. Xu X, Ray R, Gu Y, Ploehn HJ, Gearheart L, Raker K, et al. Electrophoretic analysis and purification of fluorescent single-walled carbon nanotube fragments. J Am Chem Soc 2004;126(40):12736–7. [PubMed: 15469243]
31. Cao L, Wang X, Meziani MJ, Lu FS, Wang HF, Luo PJG, et al. Carbon dots for multiphoton bioimaging. J Am Chem Soc 2007;129(37):11318–9. [PubMed: 17722926]
32. Hu SL, Niu KY, Sun J, Yang J, Zhao NQ, Du XW. One-step synthesis of fluorescent carbon nanoparticles by laser irradiation. J Mater Chem 2009;19(4):484–8.
33. Bottini M, Balasubramanian C, Dawson MI, Bergamaschi A, Bellucci S, Mustelin T. Isolation and characterization of fluorescent nanoparticles from pristine and oxidized electric arc-produced single-walled carbon nanotubes. J Phys Chem B 2006;110(2):831–6. [PubMed: 16471611]
34. Manchester S, Wang XL, Kulaots I, Gao YM, Hurt RH. High capacity mercury adsorption on freshly ozone-treated carbon surfaces. Carbon 2008;46(3):518–24. [PubMed: 19255621]
35. Criegee R. Mechanism of Ozonolysis. Angew Chem Int Edit 1975;14(11):745–52.
36. Balasubramanian K, Burghard M. Chemically functionalized carbon nanotubes. Small 2005;1(2): 180–92. [PubMed: 17193428]
37. Hemraj-Benny T, Bandosz TJ, Wong SS. Effect of ozonolysis on the pore structure, surface chemistry, and bundling of single-walled carbon nanotubes. J Colloid Interf Sci 2008;317(2):375–82.
38. Lam CW, James JT, McCluskey R, Hunter RL. Pulmonary toxicity of single-wall carbon nanotubes in mice 7 and 90 days after intratracheal instillation. Toxicol Sci 2004;77(1):126–34. [PubMed: 14514958]
39. Yang ST, Guo W, Lin Y, Deng XY, Wang HF, Sun HF, et al. Biodistribution of pristine single-walled carbon nanotubes in vivo. J Phys Chem C 2007;111(48):17761–4.
40. Jaurand MC, Renier A, Daubriac J. Mesothelioma: Do asbestos and carbon nanotubes pose the same health risk? Part Fibre Toxicol 2009;6:16. [PubMed: 19523217]
41. Martin CR, Kohli P. The emerging field of nanotube biotechnology. Nat Rev Drug Discov 2003;2 (1):29–37. [PubMed: 12509757]
42. Pastorin G. Crucial Functionalizations of Carbon Nanotubes for Improved Drug Delivery: A Valuable Option? Pharm Res-Dord 2009;26(4):746–69.

43. Kaiser JP, Krug HF, Wick P. Nanomaterial cell interactions: how do carbon nanotubes affect cell physiology? Nanomed 2009;4(1):57–63.

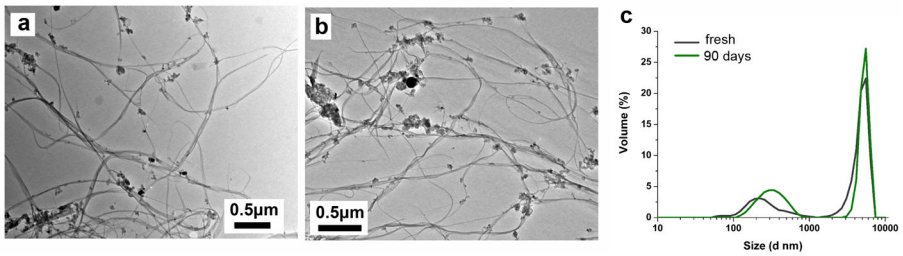

Figure 1.

Persistence and morphological stability of unfunctionalized SWCNTs upon 90 day exposure to oxidative phagolysosomal simulant. Typical TEM images before (a) and after (b) 90 day exposure, showing no detectable change. (c) Effective tube/aggregate sizes estimated by dynamic light scattering showing no detectable change over 90 days. This SWCNT sample was annealed at 1000°C prior to the experiment to reduce functional group density.

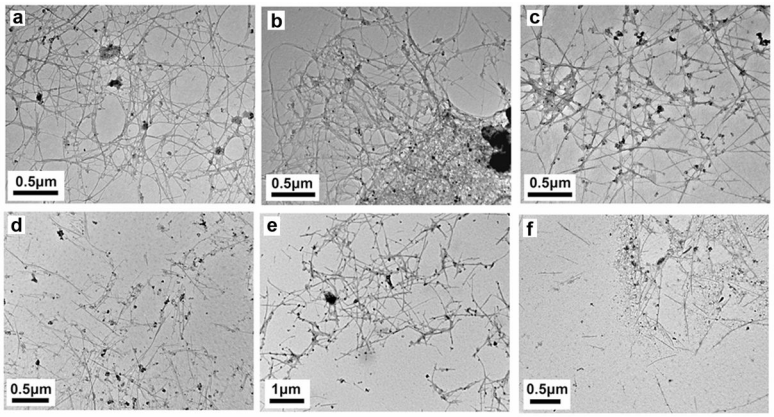

Figure 2.

Degradation and morphological instability of SWCNT-COOH upon 90 day exposure to oxidative phagolysosomal simulant. Typical TEM images before exposure (a), after 1 day (b), 7 day (c), 30 day (d), 60 day (e) and 90 day exposure (f). After 90 days the loss of the entangled rope structure and the presence of free tubes along with carbon nanoparticle debris are clearly seen.

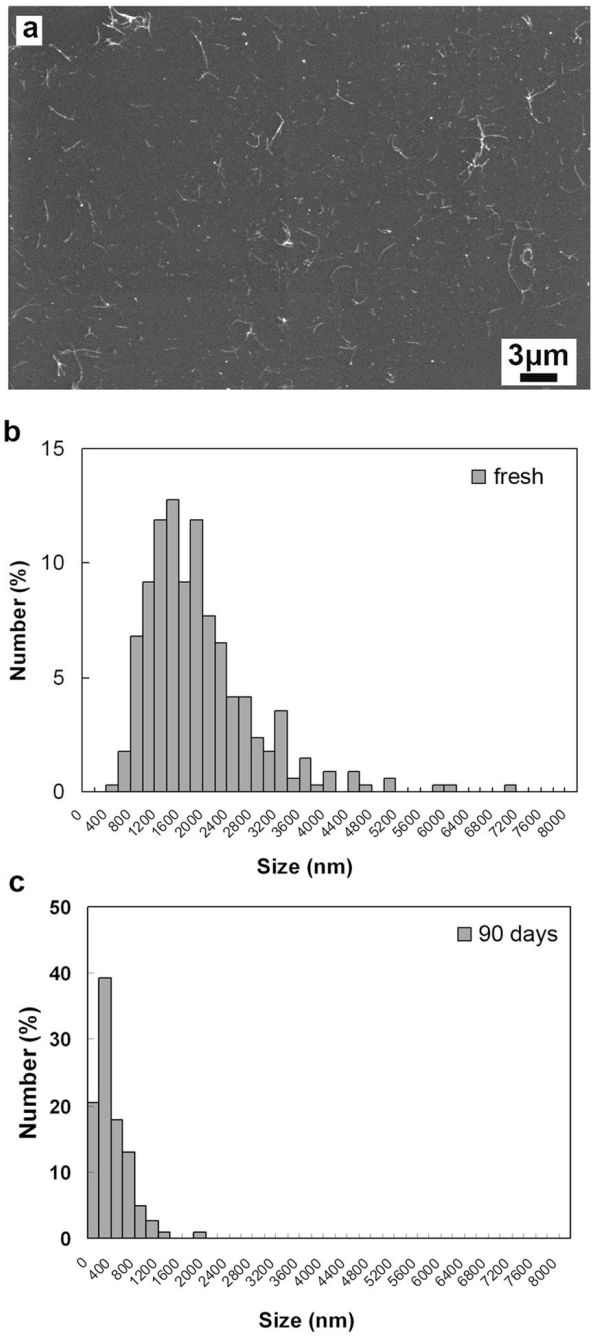

Figure 3.

Nanotube length distribution measurements for carboxylated SWCNTs before and after long-term exposure to physiological oxidizing fluids. (a) Example SEM image of fresh tubes distributed on silicon substrates by bar coating; (b, c) Nanotube length distributions determined by manual counting of about three hundred individual tubes identified on SEM micrographs. (b) SEM histogram of fresh SWCNTs-COOH shows a broad size distribution of 1940 +/− 920nm (mean +/− s.d.); (c) after 90 day exposure, length peak shifts to 419+/− 290nm, and the two mean lengths are different with a high degree of statistical significance ($p<0.0001$). (Note: the x-axes of panel b and c align for ease of comparison).

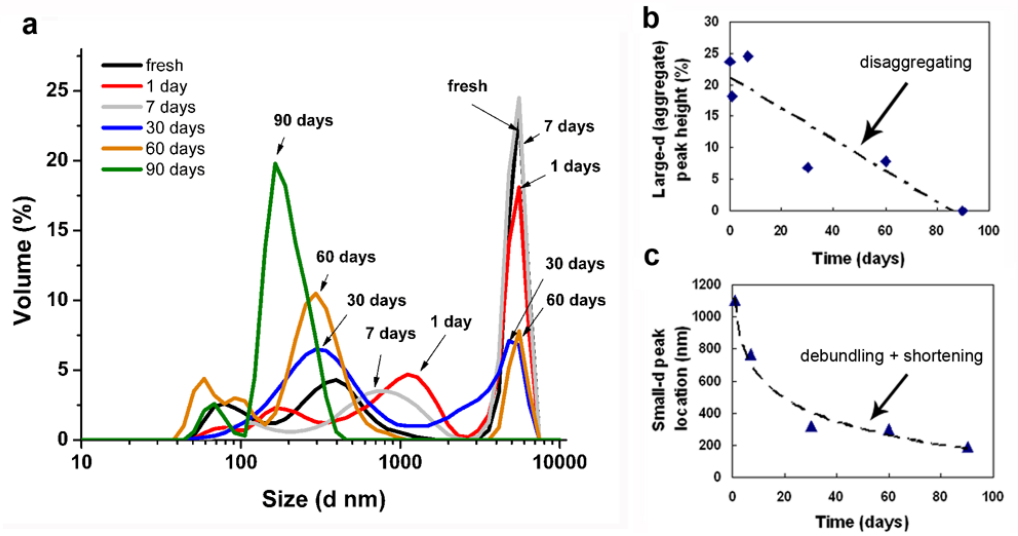

Figure 4.

Hydrodynamic size distributions by dynamic light scattering (a) show the progressive loss of the large aggregate peak and the growth of the primary tube peak over the course of 90 days. (b) quantifies the disappearance of the large aggregate peak which primarily reflects disaggregation of the rope networks, (c) quantifies the shift in the primary tube peak reflecting tube shortening by chemical degradation and debundling as well.

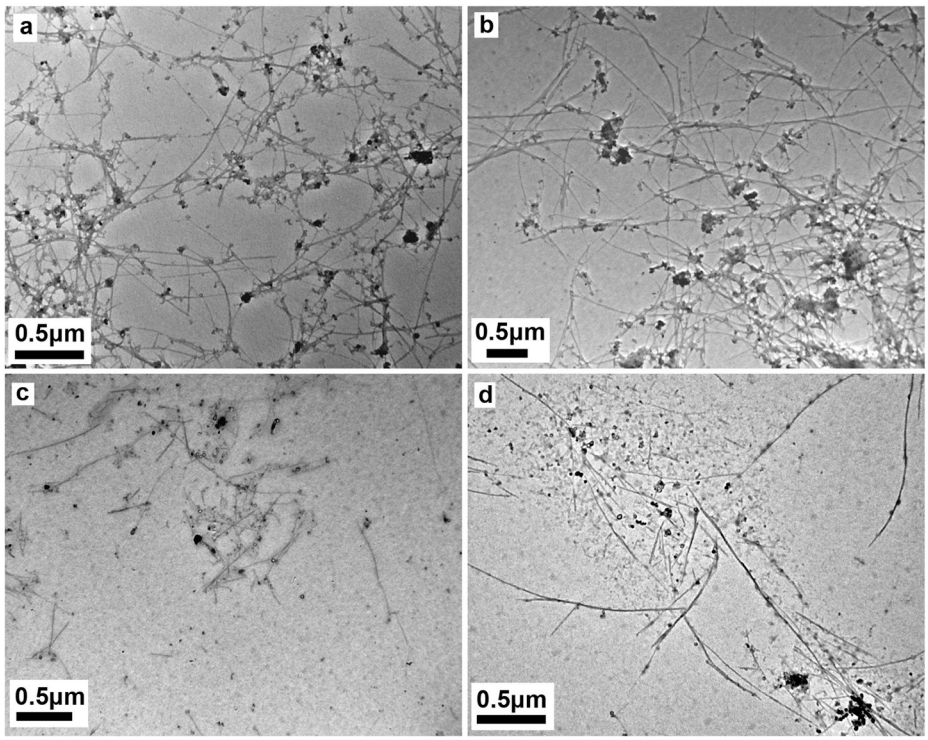

Figure 5.
Morphologies of carboxylated SWCNTs after 90 day exposure to different media: (a) DI H_2O; (b) PSF only; (c) 1mM H_2O_2 only and (d) 1mM H_2O_2 plus PSF. Tube degradation occurs only under oxidizing conditions, but does not necessarily require the low pH of the PSF buffer (pH 4.5).

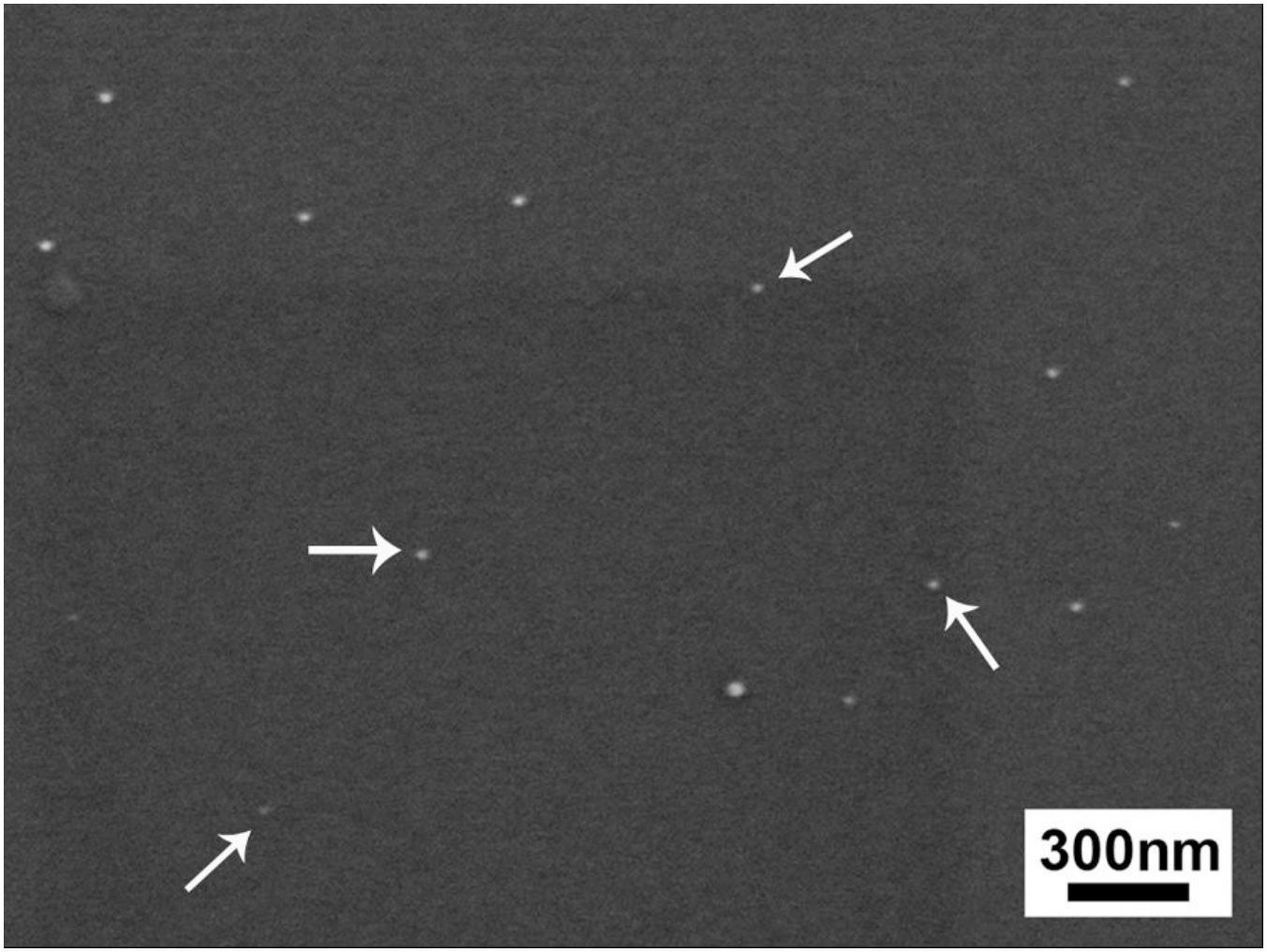

Figure 6.
SEM image showing equi-axed debris or “dots” (see arrows) on silicon substrate after 90 day exposure of carboxylated SWCNTs. The dots, which are believed to carbonaceous debris, can also be seen by close inspection of TEM images.

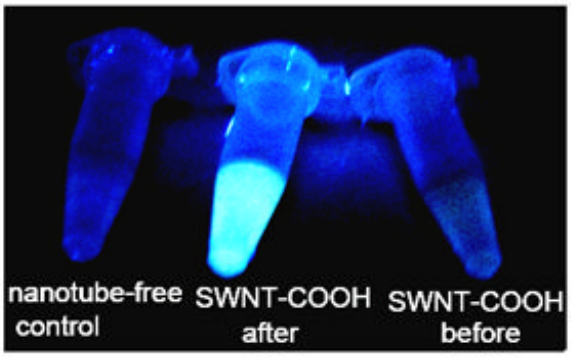

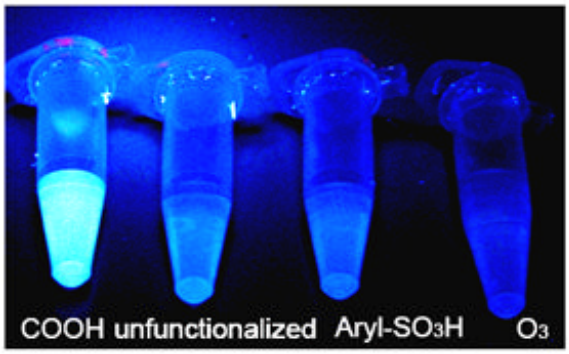

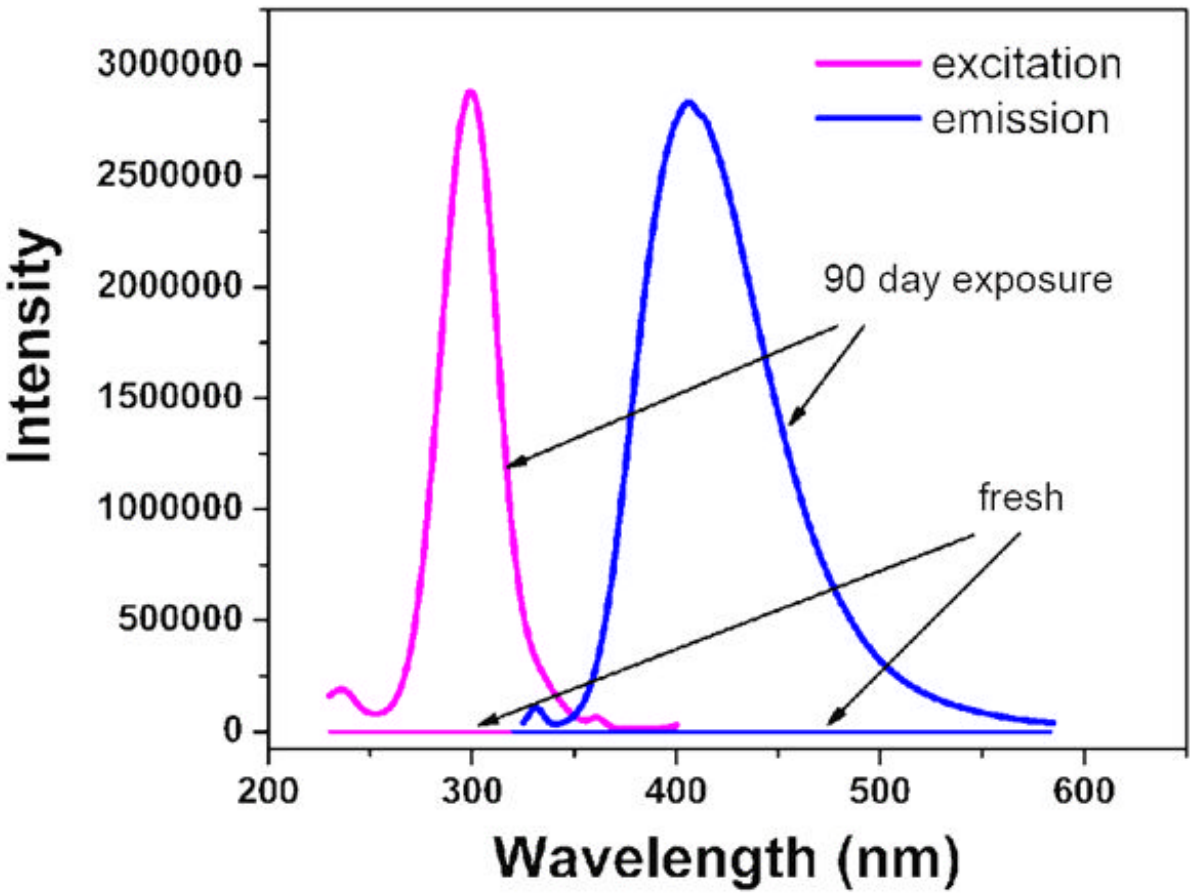

Figure 7.

Optical properties of nanotube ultra-filtrates showing evidence of < 2nm chemical degradation products in the SWCNT-COOH sample after 90-day exposure to the oxidative phagolysosomal simulant. (a) digital photograph under UV illumination showing the appearance of fluorescence in the ultra-filtrates of exposed SWCNT-COOH samples. The fluorescence is not observed in the fresh SWCNT-COOH filtrates or in the nanotube-free PSF as controls. (b) digital photographs as in (a) but for SWCNTs with different surface chemistries. Only the SWCNT-COOH sample shows the < 2nm fluorescence products. (c) Fluorescent excitation and emission spectra of ultra-filtrates form fresh and 90-day exposure SWCNT-COOH. The spectra of the fresh sample are indistinguishable from baseline.

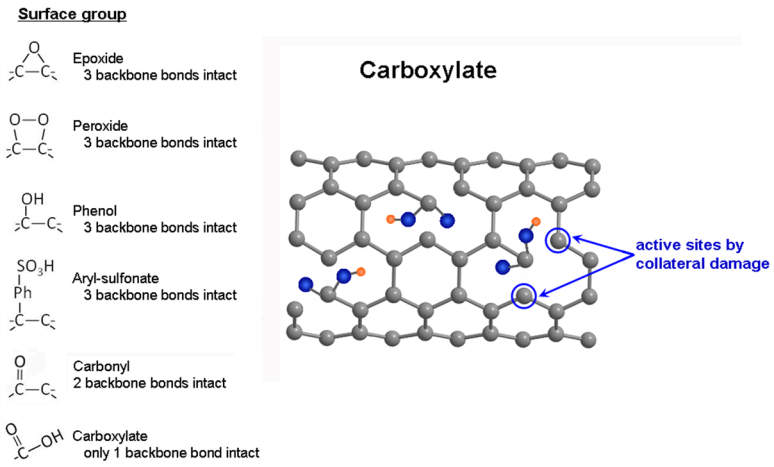

Figure 8.

Various functional groups relevant to the durability assay in this study. All groups disrupt local pi-conjugation, but carboxylation is unique in its collateral damage to the CNT backbone by creation of two active sites that provide attack points for further oxidative degradation leading to tube shortening and disentanglement.

Table 1

Nanotube and fibrous reference samples and their morphological changes after 90 day exposure to oxidizing phagolysosomal simulant

Sample	**Functionalization**	**Effect of 90 day exposure on TEM morphology**
SWCNTs (d:1–2 nm)	No functionalization	No significant change
	Aryl-sulfonation	No significant change
	Ozonolysis	No significant change
	Annealing (1000°C)	No significant change
	Carboxylation	
	Commercial (by HNO_3)	*Visible degradation*
	In-house functionalization (in HNO_3/ H_2SO_4)	
	Treatment time: 15min	No significant change
	1hr	*Visible degradation*
	3hr	*Visible degradation*
CNFs (d: 200 nm)	No functionalization	No significant change
	Aryl-sulfonation	No significant change
Wollastonite (d:53±32 nm)	No functionalization	Complete dissolution
Crocidolite Asbestos (d: 30–150nm)	No functionalization	No significant change